Bisphosphonate treatment affects trabecular bone apparent modulus through micro-architecture rather than matrix properties.

Ding, Ming

Published in:
Journal of Orthopaedic Research

Publication date:
2004

Document Version
Publisher's PDF, also known as Version of record

ELSEVIER

Journal of Orthopaedic Research 22 (2004) 465–471

Journal of Orthopaedic Research

www.elsevier.com/locate/orthres

Bisphosphonate treatment affects trabecular bone apparent modulus through micro-architecture rather than matrix properties

J.S. Day [a], M. Ding [b], P. Bednarz [a,c], J.C. van der Linden [a], T. Mashiba [d], T. Hirano [d], C.C. Johnston [d], D.B. Burr [d], I. Hvid [b], D.R. Sumner [e], H. Weinans [a,*]

[a] *Erasmus Orthopaedic Research Laboratory, Erasmus MC, University Medical Centre of Rotterdam, EE1614, P.O. Box 1738, DR, Rotterdam 3000, The Netherlands*

[b] *Orthopaedic Research Laboratory, Aarhus University Hospital, Aarhus, Denmark*

[c] *Institute of Fundamental Technological Research, Polish Academy of Sciences, Warsaw, Poland*

[d] *Department of Anatomy and Cell Biology, Indiana University School of Medicine, Indianapolis, IN, USA*

[e] *Departments of Anatomy and Cell Biology, Rush Medical College, Chicago, IL, USA*

Accepted 9 May 2003

Abstract

Bisphosphonates are emerging as an important treatment for osteoporosis. But whether the reduced fracture risk associated with bisphosphonate treatment is due to increased bone mass, improved trabecular architecture and/or increased secondary mineralization of the calcified matrix remains unclear. We examined the effects of bisphosphonates on both the trabecular architecture and matrix properties of canine trabecular bone. Thirty-six beagles were divided into a control group and two treatment groups, one receiving risedronate and the other alendronate at 5–6 times the clinical dose for osteoporosis treatment. After one year, the dogs were killed, and samples from the first lumbar vertebrae were examined using a combination of micro-computed tomography, finite element modeling, and mechanical testing. By combining these methods, we examined the treatment effects on the calcified matrix and trabecular architecture independently. Conventional histomorphometry and microdamage data were obtained from the second and third lumbar vertebrae of the same dogs [Bone 28 (2001) 524]. Bisphosphonate treatment resulted in an increased apparent Young's modulus, decreased bone turnover, increased calcified matrix density, and increased microdamage. We could not detect any change in the effective Young's modulus of the calcified matrix in the bisphosphonate treated groups. The observed increase in apparent Young's modulus was due to increased bone mass and altered trabecular architecture rather than changes in the calcified matrix modulus. We hypothesize that the expected increase in the Young's modulus of the calcified matrix due to the increased calcified matrix density was counteracted by the accumulation of microdamage.

Keywords: Bone micro-architecture; Osteoporosis; Bisphosphonates; Mechanical properties; Bone matrix mineralization

Introduction

Bisphosphonates, specific inhibitors of bone resorption, are gaining importance in the treatment of osteoporosis [7,36]. Bisphosphonates inhibit osteoclast activity on the bone surface by causing early osteoclast death, thus reducing the remodelling space, i.e., the amount of bone undergoing active remodelling at any specific time [33,35]. Bone mineral density (BMD) as measured by dual energy X-ray absorptometry is increased by increasing either the total volume of bone (bone mass) or the mineralization of the calcified bone matrix [10,27,43]. It has been demonstrated that the activation frequency (a histological measure of new resorption sites) is reduced during bisphosphonate therapy [6,28], temporarily disrupting the normal equilibrium between bone resorption and formation. Although the number of new resorption sites is reduced early in the therapy program, the existing formation sites continue to produce new bone matrix. The resultant phenomenon, known as the *bone remodelling transient,* is associated with a rapid gain in bone mass early in the treatment period. This transient behavior continues until the active remodelling sites are filled in by osteoblast activity, reducing the remodelling space until a new equilibrium is reached. The amount of bone affected by

* Corresponding author. Tel.: +31-10-40-87367/87384; fax: +31-10-40-89415.

E-mail address: h.weinans@erasmusmc.nl (H. Weinans).

0736-0266/$ - see front matter © 2003 Orthopaedic Research Society. Published by Elsevier Ltd. All rights reserved.
doi:10.1016/j.orthres.2003.05.001

the remodelling transient is determined by the change in the number and size of active remodelling units and the duration of the resorption and formation phases [15,31]. In addition to its effect on the remodelling space, the reduction in activation frequency also results in a slower equilibrium remodelling rate. Because bone turnover is reduced, the average age of the bone packets within the calcified matrix is increased. This results in increased matrix mineralization [27,34]. The therapeutic effect of the bisphosphonate alendronate is thought to be due primarily to an increase in mineralization [3,27]. While increased mineralization should result in stiffer bone material [8], concern exists that this 'frozen bone' might become brittle and/or accumulate microdamage [16,24]. Microdamage accumulation is normally prevented by remodelling, and resorption spaces can be initiated by microdamage [4,29,42]. Accumulated microdamage can contribute to a reduction of bone Young's modulus, strength, and toughness and could possibly increase fracture risk [5,44].

Recently, it has become possible to quantify the effect of changes in architecture and bone mass on the apparent mechanical behavior of bone independent of the mechanical properties of the calcified matrix. Micro-computed tomography (microCT) scanning and automated finite element (FE) methods [41] can be combined to create a powerful method for the study of treatment-induced changes in bone architecture at the trabecular level (10–20 μm). Further, changes in the Young's modulus of the calcified matrix (hereafter referred to as the matrix modulus) can be investigated by combining these methods with conventional mechanical testing [9,22]. Thus, the contributions of both matrix properties and trabecular architecture to the overall apparent modulus can be evaluated.

In this study we examined the effect of long-term treatment with high doses of two bisphosphonates, alendronate and risedronate, in a canine model. We investigated the changes induced by bisphosphonate treament to both bone architecture and matrix modulus as well as their contributions to the apparent Young's modulus. To interpret our findings, we examined the effect of bisphosphonates on remodelling, matrix mineralization, and microdamage accumulation. Specifically, we tested the hypothesis that high dose bisphosphonate treatment leads to increased secondary mineralization and consequently an increase in the matrix modulus.

Methods

Experimental design

The experimental design used in this study has been reported previously and will be briefly summarized [24]. Thirty-six female beagle dogs aged 1–2 years (control: 1.2 ± 0.4, risedronate: 1.1 ± 0.2, alendronate: 1.2 ± 0.2 (y.o. $\pm$ SD)) were divided into 3 weight matched groups. Dogs in the two treatment groups were treated daily with risedronate (Procter and Gamble Pharmaceuticals Inc., Cincinnati, OH) orally at a dose of 0.5 mg/kg/day or alendronate (Merck and Co., Inc., West Point, PA) orally at 1.0 mg/kg/day. Long-term treatment was simulated using doses that were 5–6 times higher than the clinical dose for osteoporosis. All dogs were treated for 12 months, then killed, and the first, second, and third lumbar vertebrae were removed. All procedures were in accordance with approved NIH guidelines, under a protocol approved by the Indiana University School of Medicine Animal Care and Use Committee (Study #MD 1783).

Specimen preparation: microCT and mechanical testing

One cubic trabecular bone specimen with dimensions $5 \times 5 \times 5$ mm was produced from the center of each first lumbar (L1) vertebral body, aligned with the anatomical axes in the cranial–caudal (CC), anteroposterior (AP), and medial–lateral (ML) planes. Low speed, water cooled diamond saws (EXAKT Apparatenbau, Norderstedt, Germany; Ernst Leitz Wetzlar GmbH, Wetzlar, Germany) were used for all sample preparation. Samples were stored in sealed plastic tubes at −20 °C, and care was taken to keep specimens moist during scanning and testing.

A high-resolution microCT system (μ-CT 20, Scanco Medical AG., Zürich, Switzerland) was used to scan the specimens, resulting in reconstructions with $18 \times 18 \times 18$ μm cubic voxels. The microCT images were segmented using thresholds chosen such that the volume of the dataset matched that determined physically using Archimedes' principle [12]. Archimedes' principle was also used to determine the bone volume fraction (BV/TV) and the density of the calcified matrix.

After scanning, each cubic specimen was tested in compression in an 858 Bionix MTS hydraulic material testing machine (MTS Systems Corporation, Minneapolis, MN). Specimens were tested non-destructively in compression to 6000 μstrain (apparent strain) at a strain rate of 2000 μstrain/s in the AP and ML directions to determine the apparent Young's modulus. The apparent Young's modulus of each sample was calculated as the tangent of the linear portion of the stress–strain curve at 5000 μstrain for the non-destructive tests (AP and ML directions). The specimens were then tested to failure in the CC direction with the same strain rate. The apparent Young's modulus in this direction was defined as the slope of the steepest portion of the stress–strain curve. Yield stress was defined as the intercept between the stress–strain curve and the line used to define the Young's modulus offset by 0.2% strain. Ultimate stress was defined as the peak stress encountered during testing. All testing was performed on polished platens lubricated with a low viscosity mineral oil to reduce the effect of friction [23].

Finite element models

The matrix modulus was calculated for all three directions using a combination of finite element modeling and mechanical testing. This combination was used because it enables the total apparent modulus to be partitioned into contributions due to the matrix modulus and trabecular architecture [41]. All voxel microCT data were coarsened to 36 μm, then converted to a finite element mesh of 8 node cubic elements. Coarsening was performed using a bone volume-preserving algorithm [39]. The resulting meshes typically consisted of 400,000–700,000 elements. All elements were assigned an arbitrary matrix modulus of 1 GPa and a Poisson ratio of 0.3. Boundary values were assigned to simulate an unconstrained compression test with no friction at the platens. Because we used a matrix modulus of unity with a linear finite element analysis, the apparent modulus obtained from the finite element model can simply be scaled to match the apparent modulus from each of the mechanical tests. The resulting scaling factor can be considered the matrix modulus of the sample [41]. This modulus represents the average stiffness of the voxels of the bone matrix under the assumption of homogeneous isotropic tissue properties (Fig. 1).

Simulation of increased mineralization

Bisphosphonate treatment has been previously observed to result in both increased mineralization and a loss of the normal mineralization gradient between superficial and interstitial bone [3,31,34]. We used 4

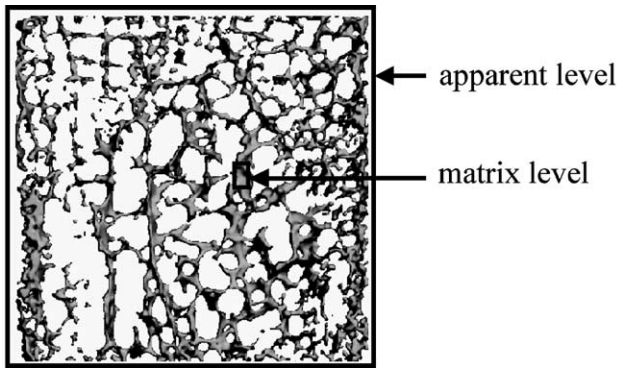

Fig. 1. Definitions of the apparent level and the matrix level. The matrix modulus was defined as the modulus effective at the scale of tens to hundreds of microns. The apparent modulus was effective at the scale of millimeters to centimeters and includes both the influence of the matrix modulus and the influence of trabecular architecture.

FE meshes from the residronate treated group to predict the effects of altered mineralization on the apparent modulus. Two conditions were simulated: homogeneous mineralization representing bisphosphonate treated bone and a heterogenous mineralization that was more representative of normal bone with lower mineralization at the surface and higher mineralization of the interstitial bone [40]. To accomplish the simulations, an image erosion algorithm was used to identify bone voxels within 36 μm of the surface. A 5% increase in total mineralization was assumed for the bisphosphonate treated samples [3,28,34]. By assuming that bisphosphonate treatment mostly affected surface voxels, a lower relative mineralization was calculated for the normal surface voxels. We then used either a linear or cubic relation as the extreme boundaries for the relation between mineral content and Young's modulus [8]. After solving the FE models we compared the apparent modulus in the CC direction for the normal (inhomogeneous properties) and the treated (homogeneous properties) models.

Histomorphometry and microdamage

Dynamic histomorphometry and microdamage data from the second and third lumbar vertebrae respectively were obtained from a previous study of the same animals. The following parameters were used in the current paper to aid interpretation of the results: activation frequency (Ac.F), bone formation rate/bone surface (BFR/BS), osteoid surface/bone surface (OS/BS), crack number (Cr.N), crack length (Cr.Le), crack density (Cr.Dn), and crack surface density (Cr.S.Dn) [25].

Statistical analysis

The statistical analyses included two-way analyses of variance for repeated measures for the experimental apparent modulus, apparent modulus predicted by the FE models, and matrix modulus. The group (normal, risedronate, or alendronate) was used as the between-subjects factor and testing direction (cranial–caudal, anterior–posterior, medial–lateral) as the within-subjects factor. Bone volume fraction, matrix density, histomorphometric parameters, and microdamage parameters were analyzed using standard analysis of variance. When significant main effects were found, specific comparisons were made with Dunnett two-sided t-tests. In all cases, the exact p-values are given; we considered $p < 0.05$ to represent significant effects.

A stepwise multiple regression analysis was used to assess the suitability of the FE models for the prediction of the apparent modulus measured in three directions in the laboratory. In this model the dependent variable was the measured apparent modulus and the independent variables were apparent modulus predicted by FE, testing direction, and the treatment group. Correlation analysis was used to examine the relations between the matrix density, matrix modulus, and both remodelling and microdamage parameters. Statistical analyses were performed using SPSS version 8.0 (SPSS Inc., Chicago, IL, USA).

Results

One dog was excluded due to distemper at the start of treatment, and one vertebra was destroyed during preparation. This left 11 control, 11 risedronate-treated, and 12 alendronate-treated dogs. Bisphosphonate treatment resulted in an increase in the bone volume fraction and calcified matrix density as determined using Archimedes' principle. The increase of approximately 2% in matrix density was significant for both treatments, but the change in BV/TV was only significant for the risedronate group where the increase was 18% (Table 1).

The experimentally measured apparent modulus was affected by bisphosphonate treatment ($p = 0.001$). A significant effect of direction ($p < 0.001$) and an

Table 1
Results for one-way ANOVA

	Control	Risedronate	Alendronate	ANOVA	Control vs. Risedronate	Control vs. Alendronate
BV/TV	0.22 [0.20, 0.24]	0.26 [0.23, 0.28]	0.23 [0.22, 0.24]	0.009	0.007	0.657
ρ_{matrix} (g/cc)	2.09 [2.08, 2.11]	2.14 [2.11, 2.16]	2.13 [2.12, 2.14]	0.005	0.005	0.013
$\sigma_{ultimate\ (MPa)}$	8.3 [6.9, 9.6]	11.4 [10.4, 12.3]	9.8 [8.6, 10.9]	0.008	0.004	0.120
$\sigma_{yield\ (MPa)}$	7.4 [6.1, 8.7]	10.2 [9.4, 11.0]	8.9 [8.0, 9.8]	0.004	0.002	0.070
Ac.F ($year^{-1}$)	1.65 [0.33, 4.18]	0.18 [0.03, 0.60]	0.09 [0.024, 0.16]	0.000	0.000	0.000
BFR/BS ($\mu m^3/\mu m^2$/year)	80.0 [18.6, 152.2]	10.5 [1.1, 36.9]	5.5 [1.4, 11.7]	0.000	0.000	0.000
OS/BS (%)	8.5 [5.8, 11.2]	1.5 [0.7, 2.2]	1.0 [0.6, 1.3]	0.000	0.000	0.000
Cr.N (#)	0.7 [0.3, 1.2]	3.3 [1.5, 5.0]	3.7 [2.8, 4.5]	0.001	0.003	0.001
Cr.Le (μm)	39.2 [22.3, 56.2]	49.4 [31.4, 67.4]	45.7 [40.6, 50.9]	0.557	–	–
Cr.Dn (#/mm^2)	0.33 [0.11, 0.54]	0.80 [0.41, 1.19]	1.19 [0.88, 1.51]	0.001	0.052	0.000
Cr.S.Dn (μm/mm^2)	11.6 [3.8, 19.5]	39.8 [19.5, 60.0]	53.1 [39.8, 66.3]	0.000	0.011	0.000

Mean values and 95% confidence intervals are presented on the left for histomorphometry (top), mechanical properties (middle), matrix density (middle: ρ_{matrix}), and microdamage (bottom). On the right p-values are presented for both the ANOVA and the posthoc tests.

interaction between direction and treatment ($p = 0.018$) were found. On average, the risedronate treated group was 37% stiffer than the control group ($p = 0.001$). No significant difference was found in the alendronate group ($p = 0.215$; Fig. 2A). The apparent modulus predicted by the FE models (contribution of trabecular architecture and bone mass) was also affected by bisphosphonate treatment ($p = 0.001$) with effects similar to the mechanical tests (Fig. 2B). As in the mechanical testing, there was a significant effect of direction ($p < 0.001$), but no interaction between direction and treatment ($p = 0.246$). The predicted apparent modulus in the risedronate group was approximately 40% higher than the control group ($p < 0.001$). No significant effect of alendronate treatment was found ($p = 0.283$; Fig. 2B). The matrix modulus was not significantly affected by treatment ($p = 0.517$), nor was there significant interaction between direction and treatment group ($p = 0.893$). Direction significantly affected the matrix modulus, which was 20–30% larger in the CC than in the AP or ML directions ($p < 0.001$; Fig. 2C). Bisphosphonate treatment resulted in an increase in both the ultimate stress and the yield stress. However, after correcting for architecture, this difference was not significant (Table 1).

In the multiple regression analysis, the FE models (i.e., effect of architecture and bone mass) accounted for 89.3% ($p < 0.0001$) of the variance in the experimentally measured modulus. A small architecture independent effect of direction was found, which contributed to 0.5% of the variance ($p = 0.04$). Treatment group and direction-group interaction were not significant. The residual variance was 10.2%.

To estimate the statistical power of our results, we simulated the predicted effect of increased mineralization on the matrix modulus. We assumed an increase of 5% in the mineralization of the bisphosphonate treated group. For bone with a mineral fraction of approximately 40%, this agreed well with our observed matrix density measurements. Based on the simulations we predicted that the matrix modulus should increase by between 5% (conservative linear model) and 14% (cubic model) in the treated animals. From these simulations we could estimate that, for the sample size used, the power (β) to detect a difference in the group mean matrix modulus with a two-sided t-test ($\alpha = 0.05$) was between 0.12 (for the conservative linear model) and 0.65 (for the cubic model). Because of the limited power of our results, care must be taken when comparing the group means for matrix modulus.

Because one sample from the control group was destroyed during preparation, we reworked our previous data [25], which are included in Table 1. From these data a large significant decrease in bone remodelling activity is apparent in the bisphosphonate treated groups, as well as an increased microdamage burden in the treated animals as indicated by significant increases in Cr.N, Cr.Dn and Cr.S.Dn.

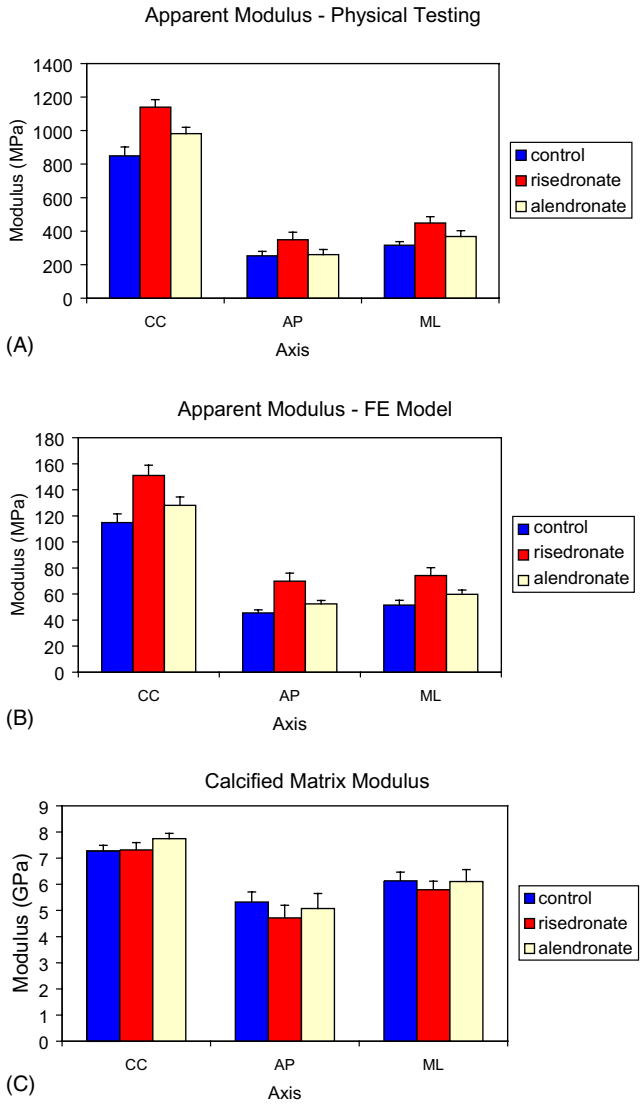

Fig. 2. Mechanical testing and FE simulation results. Cubes of trabecular bone from the first lumbar vertebra were tested in three directions in compression (Fig. 2A). FE models with a matrix modulus of 1 GPa were used to quantify the contribution of trabecular architecture (Fig. 2B). The mineralized matrix modulus was the scaling factor between the physical tests and the FE simulated results (Fig. 2C). Testing directions were cranial–caudal (CC), anteroposterior (AP) and medial–lateral (ML). Results (mean + SEM) are grouped by test direction on the x-axis of each graph. Treatment group is indicated by the shading of the bars. (A): Apparent Young's modulus from physical testing. Two-way ANOVA indicated an effect of treatment ($p = 0.015$) and direction ($p < 0.001$). Risedronate treated samples were significantly stiffer than the control group ($p = 0.012$). (B): Relative modulus calculated using FE models. Two-way ANOVA indicated an effect of treatment ($p = 0.001$) and direction ($p < 0.001$). The simulated apparent modulus of risedronate treated samples was significantly stiffer than the control group ($p =< 0.001$). (C): Matrix modulus. Bisphosphonate treatment had no effect on the matrix modulus ($p = 0.699$). There was an effect of direction ($p < 0.001$).

Linear regression analysis revealed that the matrix density was significantly correlated to both the remodelling (ES/BS $r = -0.555$, $p = 0.001$; OS/BS $r = -0.594$, $p < 0.001$; BFR/BV $r = 0.487$, $p = 0.004$; Ac.F $r = -0.353$, $p = 0.044$) and microdamage parameters (Cr.N $r = 0.456$, $p = 0.007$; Cr.Dn $r = 0.412$, $p = 0.015$; Cr.S.Dn $r = 0.511$, $p = 0.002$). The matrix modulus, however, was not significantly correlated to the matrix density, remodelling, or microdamage parameters.

Discussion

The major purpose of this study was to determine whether the increased levels of matrix mineralization seen after long-term bisphosphonate therapy affected the matrix mechanical properties. We used a high dose to simulate long-term effects in the bone. Bone remodelling was greatly reduced, resulting in both a 2% increase in the matrix density (indicative of increased mineralization) and increased microdamage accumulation. By using a combination of FE modelling, microCT scanning, and mechanical testing, we investigated the effects of treatment on the apparent Young's modulus, bone architecture, and calcified matrix properties. A significant increase of the apparent modulus was observed in the risedronate treated group. This increase was predicted by the FE models, indicating a strong effect of trabecular architecture and bone mass. The importance of architecture was further indicated by the results of the multiple regression analysis where 89.3% of the variance in the mechanical testing was accounted for by the FE models with no independent effect of treatment group (an effect of treatment group would indicate a group specific difference independent of the FE results, i.e., matrix modulus). Although the matrix density was increased, there were no significant differences in the group mean matrix moduli.

A limitation of our study design is that we used intact, 'normal' dogs. In an osteoporotic population bone turnover is likely increased, resulting in lower mean mineralization of the calcified matrix. Hypomineralization in an osteoporotic population could lead to a decrease of the matrix modulus compared to the 'normal' population used in this study.

Using microCT scans to create trabecular level FE models requires that the scan be of sufficient resolution and quality to resolve individual trabeculae accurately. Our use of 36 μm voxels and individual thresholds was sufficient to create accurate meshes [30]. We found an average matrix modulus of 5.9 GPa, well within the range previously reported using this method [9,18,38,41]. Initially, we were concerned that the reduction in the amount of osteoid in the bisphosphonate treated groups could bias our segmentation of the CT data. Calculations indicated that the quantity of unmineralized osteoid tissue was not large enough to influence the choice of thresholds (data not shown). Further, we found no significant relation between OS/BS and matrix modulus ($0.41 \leqslant p \leqslant 0.72$ for Pearson correlation depending on direction) and concluded that this factor had little or no effect on the model results.

We found that the matrix modulus was influenced by the testing direction (Fig. 2C). This could be due to preferential loss of material due to thresholding in the presence of strong anisotropy at the trabecular level [20], non-ideal behavior (i.e. buckling of trabeculae) that is not represented in the FE model's boundary conditions [17,19], non-ideal behavior of the model's linear brick-shaped elements [21], or true material anisotropy at the sub-trabecular level [32].

Clinically a large increase in BMD has been observed in the first year of antiresorptive therapy. Following this, BMD either slowly increases or reaches a plateau [26,37]. It was believed that the initial gain in BMD was indicative of an increase in bone mass due to the transient change in remodelling space and that the later gain in BMD was the result of increased mineralization. It has recently been suggested that increased secondary mineralization, rather than bone mass, is responsible for the reduced fracture risk after alendronate therapy [3]. In a two-year clinical study of alendronate therapy, the authors observed an increase in spinal BMD, but no significant increase in bone mass in transiliac biopsies. Analysis of the biopsies by contact microradiography revealed 9.3% and 7.3% increases in the mean degree of mineralization of cortical and trabecular bone, respectively. Based on these findings, the authors concluded that the reduction of fracture incidence was due to secondary mineralization rather than increased bone mass. This contradicts a previous study of ovariectomized primates where an increase in the bone volume fraction was measured after two years of treatment with alendronate as compared to saline vehicle treated animals [1]. The extrapolation of results obtained from iliac biopsies to spine BMD as measured by DEXA is tenuous as this study was underpowered to detect differences in the iliac crest. Also, large differences in remodelling can exist between the spine and iliac crest [13].

While it is logical that normalizing the mineralization of hypomineralized bone in osteoporotics to normal levels should be beneficial to the patient, the exclusion of the contribution of increased bone mass is not supported by our data. Although we predicted an increase of at least 5% for the matrix modulus based on our measurements of increased matrix density, we observed only small insignificant changes in the moduli of the calcified matrix in the bisphosphonate treated groups (5% decrease in risedronate treated group and a 1% increase in the alendronate treated group; Fig. 2C).

Based on our data, we conclude that the increased apparent modulus seen in bisphosphonate therapy

results from increased bone mass and altered trabecular architecture. This is supported by a concurrent study of the three-dimensional morphology of specimens from the same animals [11]. Our results are in agreement with the clinical data, where the greatest reduction in fracture risk occurs during the first year of treatment, but fewer fractures are also found in subsequent years compared to placebo treated controls [2,10,14]. It would seem likely that reduction of fracture risk seen clinically in bisphosphonate therapy is the result of the increase in bone mass early in the treatment as the remodelling space is 'filled in'. Further increase in BMD through secondary mineralization could provide some benefit in the short term at clinical doses but may be harmful to the patient in the long term as microdamage accumlates. In the present study there was a significant positive correlation between tissue density and microdamage accumulation. We speculate that increased matrix mechanical properties due to mineralization may have been obscured by increased microdamage. Therefore, clinical dosing regimens should be chosen carefully to ensure adequate bone turnover.

Acknowledgements

Support for this work was received from NIH grants 2 PO1 AG05793-12, AR46225, and AR39239 and the Danish Health Research Council grant 9601833_lpa. Computing time was provided by The Netherlands Computing Facility (NWO/NCF). Jacqueline van der Linden was supported by the Dutch Foundation for Research (NWO/MW). The authors wish to thank Mary Hooser, Diana Jacob, and Thurman Alvey for histological preparation, Jian-Hua Hu for preparation of the samples for mechanical testing, and Paul Mulder of NIHES for statistical assistance. Merck and Co., Inc. and Procter and Gamble Pharmaceuticals Inc. kindly supplied the bisphosphonates.

References

[1] Balena R, Toolan BC, Shea M, Markatos A, Myers ER, Lee SC, et al. The effects of 2-year treatment with the aminobisphosphonate alendronate on bone metabolism, bone histomorphometry, and bone strength in ovariectomized nonhuman primates. J Clin Invest 1993;92:2577–86.

[2] Black DM, Cummings SR, Karpf DB, Cauley JA, Thompson DE, Nevitt MC, et al. Randomised trial of effect of alendronate on risk of fracture in women with existing vertebral fractures Fracture Intervention Trial Research Group. Lancet 1996;348:1535–41.

[3] Boivin GY, Chavassieux PM, Santora AC, Yates J, Meunier PJ. Alendronate increases bone strength by increasing the mean degree of mineralization of bone tissue in osteoporotic women. Bone 2000;27:687–94.

[4] Burr DB, Martin RB, Schaffler MB, Radin EL. Bone remodelling in response to in vivo fatigue microdamage. J Biomech 1985;18:189–200.

[5] Burr DB, Turner CH, Naick P, Forwood MR, Ambrosius W, Hasan MS, et al. Does microdamage accumulation affect the mechanical properties of bone? J Biomech 1998;31:337–45.

[6] Chavassieux PM, Arlot ME, Reda C, Wei L, Yates AJ, Meunier PJ. Histomorphometric assessment of the long-term effects of alendronate on bone quality and remodelling in patients with osteoporosis. J Clin Invest 1997;100:1475–80.

[7] Crandall C. Risedronate: a clinical review. Arch Intern Med 2001;161:353–60.

[8] Currey JD. Effects of differences in mineralization on the mechanical properties of bone. Philos Trans R Soc Lond B Biol Sci 1984;304:509–18.

[9] Day JS, Ding M, van der Linden JC, Hvid I, Sumner DR, Weinans H. A decreased subchondral trabecular bone tissue elastic modulus is associated with pre-arthritic cartilage damage. J Orthop Res 2001;19:914–8.

[10] Delmas PD. How does antiresorptive therapy decrease the risk of fracture in women with osteoporosis? Bone 2000;27:1–3.

[11] Ding M, Day JS, Burr DB, Mashiba T, Hirano T, Weinans H, et al. Canine cancellous bone microarchitecture after one year of high-dose bisphosphonates. Calcif Tissue Int 2003;72:737–44.

[12] Ding M, Odgaard A, Hvid I. Accuracy of cancellous bone volume fraction measured by micro-CT scanning. J Biomech 1999;32:323–6.

[13] Eventov I, Frisch B, Cohen Z, Hammel I. Osteopenia, hematopoiesis, and bone remodelling in iliac crest and femoral biopsies: a prospective study of 102 cases of femoral neck fractures. Bone 1991;12:1–6.

[14] Harris ST, Watts NB, Genant HK, McKeever CD, Hangartner T, Keller M, et al. Effects of risedronate treatment on vertebral and nonvertebral fractures in women with postmenopausal osteoporosis: a randomized controlled trial Vertebral Efficacy With Risedronate Therapy (VERT) Study Group. Jama 1999;282:1344–52.

[15] Heaney RP. The bone-remodelling transient: implications for the interpretation of clinical studies of bone mass change. J Bone Miner Res 1994;9:1515–23.

[16] Hirano T, Turner CH, Forwood MR, Johnston CC, Burr DB. Does suppression of bone turnover impair mechanical properties by allowing microdamage accumulation? Bone 2000;27:13–20.

[17] Jacobs CR, Davis BR, Rieger CJ, Francis JJ, Saad M, Fyhrie DP. NACOB presentation to ASB Young Scientist Award: Postdoctoral. The impact of boundary conditions and mesh size on the accuracy of cancellous bone tissue modulus determination using large-scale finite-element modeling North American Congress on Biomechanics J Biomech 1999;32:1159–64.

[18] Kabel J, van Rietbergen B, Dalstra M, Odgaard A, Huiskes R. The role of an effective isotropic tissue modulus in the elastic properties of cancellous bone. J Biomech 1999;32:673–80.

[19] Keaveny TM, Pinilla TP, Crawford RP, Kopperdahl DL, Lou A. Systematic and random errors in compression testing of trabecular bone. J Orthop Res 1997;15:101–10.

[20] Kuhn JL, Goldstein SA, Feldkamp LA, Goulet RW, Jesion G. Evaluation of a microcomputed tomography system to study trabecular bone structure. J Orthop Res 1990;8:833–42.

[21] Ladd AJ, Kinney JH. Numerical errors and uncertainties in finite-element modeling of trabecular bone. J Biomech 1998;31:941–5.

[22] Ladd AJ, Kinney JH, Haupt DL, Goldstein SA. Finite-element modeling of trabecular bone: comparison with mechanical testing and determination of tissue modulus. J Orthop Res 1998;16:622–8.

[23] Linde F, Hvid I. The effect of constraint on the mechanical behaviour of trabecular bone specimens. J Biomech 1989;22:485–90.

[24] Mashiba T, Hirano T, Turner CH, Forwood MR, Johnston CC, Burr DB. Suppressed bone turnover by bisphosphonates increases microdamage accumulation and reduces some biomechanical properties in dog rib. J Bone Miner Res 2000;15:613–20.
[25] Mashiba T, Turner CH, Hirano T, Forwood MR, Johnston CC, Burr DB. Effects of suppressed bone turnover by bisphosphonates on microdamage accumulation and biomechanical properties in clinically relevant skeletal sites in beagles. Bone 2001;28:524–31.
[26] McClung MR. Current bone mineral density data on bisphosphonates in postmenopausal osteoporosis. Bone 1996;19:195S–8S.
[27] Meunier PJ, Boivin G. Bone mineral density reflects bone mass but also the degree of mineralization of bone: therapeutic implications. Bone 1997;21:373–7.
[28] Monier-Faugere MC, Geng Z, Paschalis EP, Qi Q, Arnala I, Bauss F, et al. Intermittent and continuous administration of the bisphosphonate ibandronate in ovariohysterectomized beagle dogs: effects on bone morphometry and mineral properties. J Bone Miner Res 1999;14:1768–78.
[29] Mori S, Burr DB. Increased intracortical remodelling following fatigue damage. Bone 1993;14:103–9.
[30] Niebur GL, Yuen JC, Hsia AC, Keaveny TM. Convergence behavior of high-resolution finite element models of trabecular bone. J Biomech Eng 1999;121:629–35.
[31] Parfitt AM. The composition, structure and remodelling of bone: a basis for interpretation of bone mineral measurements, in: Dequeker J, Geusens P, Wahner HW, editors. Bone mineral measurement by photon absorptiometry. Leuven: Leuven University Press; 1988.
[32] Rho JY, Roy 2nd ME, Tsui TY, Pharr GM. Elastic properties of microstructural components of human bone tissue as measured by nanoindentation. J Biomed Mater Res 1999;45:48–54.
[33] Rodan GA, Fleisch HA. Bisphosphonates: mechanisms of action. J Clin Invest 1996;97:2692–6.
[34] Roschger P, Fratzl P, Klaushofer K, Rodan G. Mineralization of cancellous bone after alendronate and sodium fluoride treatment: a quantitative backscattered electron imaging study on minipig ribs. Bone 1997;20:393–7.
[35] Russell RG, Rogers MJ. Bisphosphonates: from the laboratory to the clinic and back again. Bone 1999;25:97–106.
[36] Siris E. Alendronate in the treatment of osteoporosis: a review of the clinical trials. J Womens Health Gend Based Med 2000;9:599–606.
[37] Tonino RP, Meunier PJ, Emkey R, Rodriguez-Portales JA, Menkes CJ, Wasnich RD, et al. Skeletal benefits of alendronate: 7-year treatment of postmenopausal osteoporotic women. Phase III osteoporosis treatment study group. J Clin Endocrinol Metab 2000;85:3109–15.
[38] Ulrich D, Hildebrand T, Van Rietbergen B, Muller R, Ruegsegger P. The quality of trabecular bone evaluated with micro-computed tomography, FEA and mechanical testing. Stud Health Technol Inform 1997;40:97–112.
[39] Ulrich D, van Rietbergen B, Weinans H, Ruegsegger P. Finite element analysis of trabecular bone structure: a comparison of image-based meshing techniques. J Biomech 1998;31:1187–92.
[40] Van Der Linden JC, Birkenhager-Frenkel DH, Verhaar JA, Weinans H. Trabecular bone's mechanical properties are affected by its nonuniform mineral distribution. J Biomech 2001;34:1573–80.
[41] van Rietbergen B, Weinans H, Huiskes R, Odgaard A. A new method to determine trabecular bone elastic properties and loading using micromechanical finite-element models. J Biomech 1995;28:69–81.
[42] Verborgt O, Gibson GJ, Schaffler MB. Loss of osteocyte integrity in association with microdamage and bone remodelling after fatigue in vivo. J Bone Miner Res 2000;15:60–7.
[43] Weinstein RS. True strength. J Bone Miner Res 2000;15:621–5.
[44] Zioupos P. Accumulation of in vivo fatigue microdamage and its relation to biomechanical properties in ageing human cortical bone. J Microsc 2001;201:270–8.